Image-space wave-equation tomography with image-space phase-encoded wavefields: Field data example

Claudio Guerra

ABSTRACT

In SEP, the 3D Elf-North Sea dataset has been used in projects involving the definition of depth-migration velocity. Here, I show the first 2D results of field data using image-space phase-encoded wavefields as input to the wave-equation tomography in the image space. In addition, the common-azimuth 3D migration with the initial velocity model has been started on CEES computers (cees-opteron).

INTRODUCTION

I present field data results of using image-space phase-encoded wavefields (ISPEW) in the image-space wave-equation tomography (ISWET). The field dataset is taken from the in-line 2500 of the 3D-Elf North-Sea, which has been submitted to azimuth-moveout correction (AMO). The goal is to evaluate the issues of using ISPEW on field data to define the velocity model to support the oncoming application to the entire 3D data.

The comparison of the results with the ones obtained with the inital velocity and with the original velocity show that the final optimized velocity model is reasonably accurate.

2D-PROCESSING FLOW

The 3D Elf-North Sea dataset was submitted to AMO to be subsequently migrated with common-azimuth migration. Therefore, its dimensions are given in number of in-lines, cross-lines, source-receiver offsets and frequency. It is composed of 216 in-lines, 672 cross-lines, 72 offsets with interval of 50 m and 360 frequencies. The in-line and cross-line intervals are 20 m. I selected in-line 2500 from the 3D dataset; the seismic data was sorted back to the shot domain and it had its offsets and shot interval interpolated to 25 m. A split-spread geometry was generated using reciprocity. Eight-one plane-wave areal shots were computed. They are used in the initial and intermediate migrations, on which results target horizons were interpreted.

The top of the chalk layer was interpreted on a 2D section migrated with the original velocity model. This interface is the upper-limit of the region where the original velocity model (Figure 1) was edited to generate the initial velocity model. Above it, the original velocity is unchanged. The initial velocity model(Figure 2) was obtained by smoothing and scaling the vertical slice at in-line 2500 of the original 3D velocity model computed with ray-tracing tomography. The interval slowness ratio between the original and initial velocity models ranges form 0.1 to 0.3 (Figure 3).

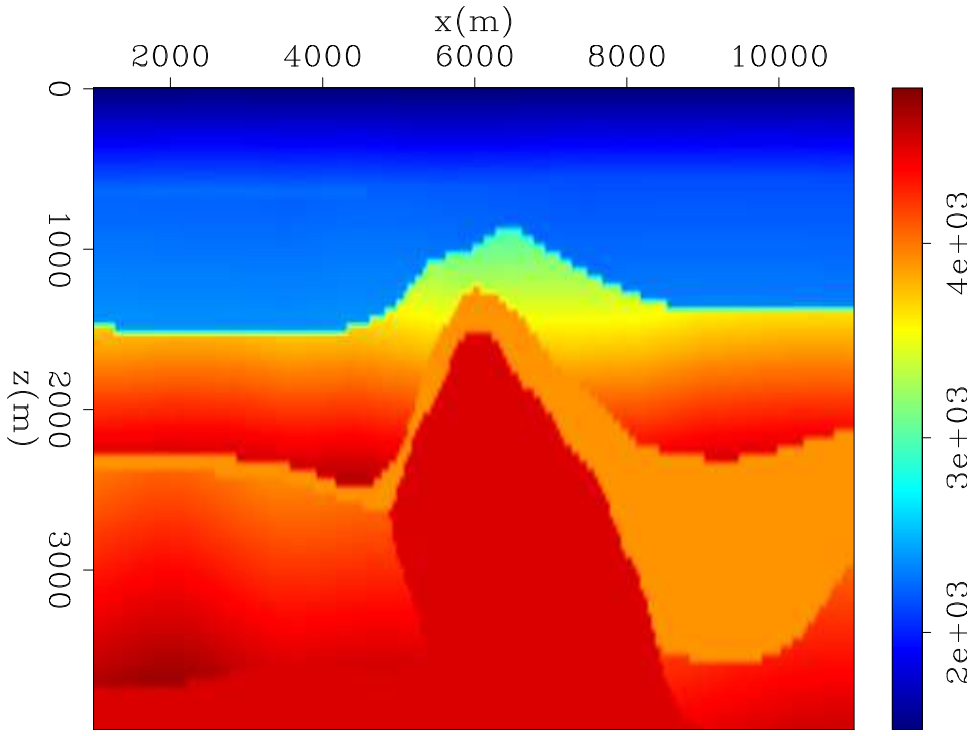

Figure 1: Original velocity model taken from a 3D velocity model computed with 3D ray-based tomography at the vertical slice conrresponding to in-line 2500.

Velocity update

Initially, a quasi-Newton optimization scheme with the L-BFGS algorithm **?** was used to perform the non-linear update of the velocity model. Differently from the example with synthetic data in which it performed satisfactorily **?**, the algorithm was not able to provide a useful velocity update. Even though the objective function decreased during the initial iterations, it gradually moved back to the value computed with the initial model during the subsequent iterations. This behavior is not completely understood and deserves further analysis. Therefore, a simple bounded steepest-descent algorithm with parabolic line-search was coded for the velocity optimization.

The entire velocity update can be summarized according to the flowchart of Figure 4. The gray box corresponds to iterations of modeling image-space phase-encoded

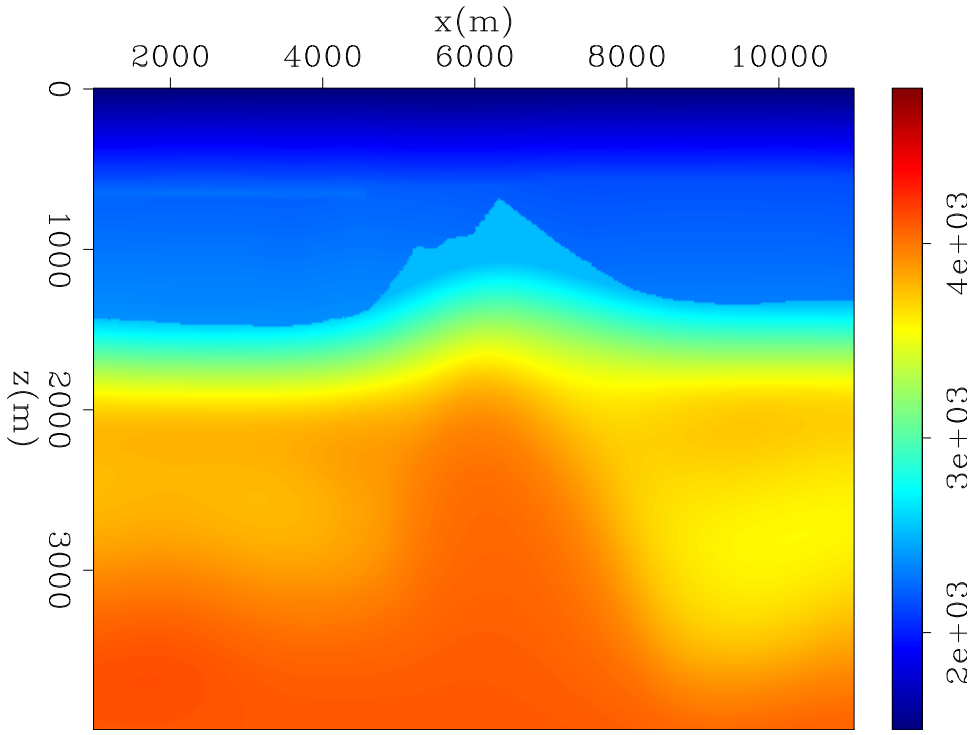

Figure 2: Initial velocity model obtained by editing the original velocity model of Figure 1.

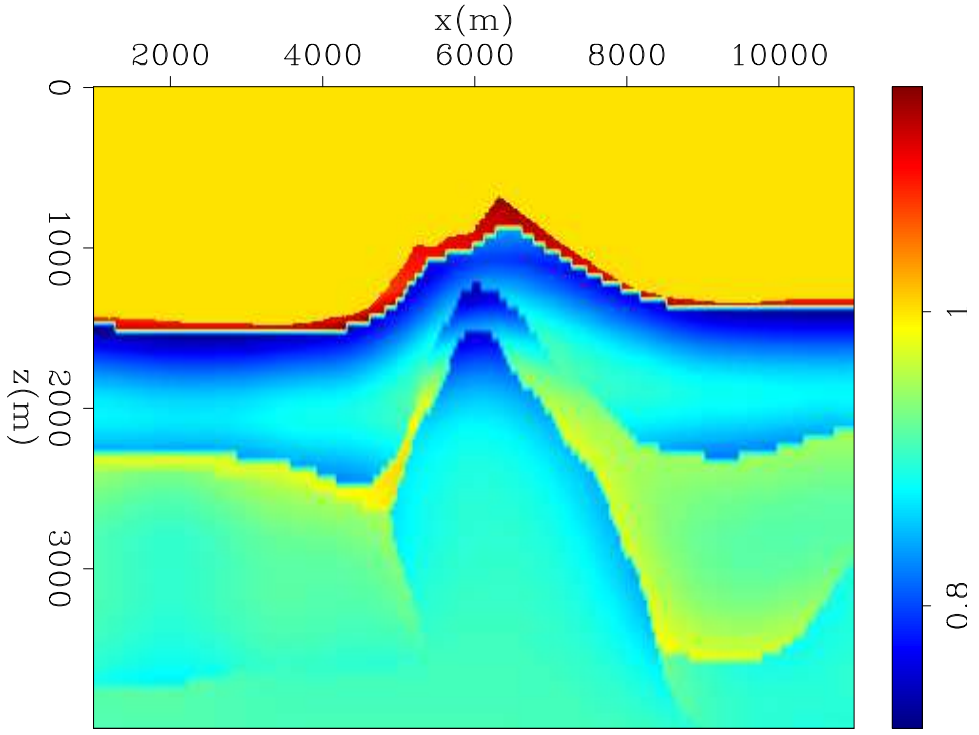

Figure 3: Velocity ration between the original and the initial velocity.

wavefields and velocity model update. Three iterations were performed, corresponding to the velocity update of the chalk layer and two additional layers below. With a satisfactory velocity model for the sediment portion, the right flank of the salt body and its top were interpreted and used as reference to generate a new velocity model with salt flooding. After plane-wave migration with this new velocity model, salt overhang on the left and its base were picked and used to finally delineate the salt body (Figure 5). This is considered the final velocity model because due to poor angular coverage in the deeper levels velocity updates are not reliable. For the velocity

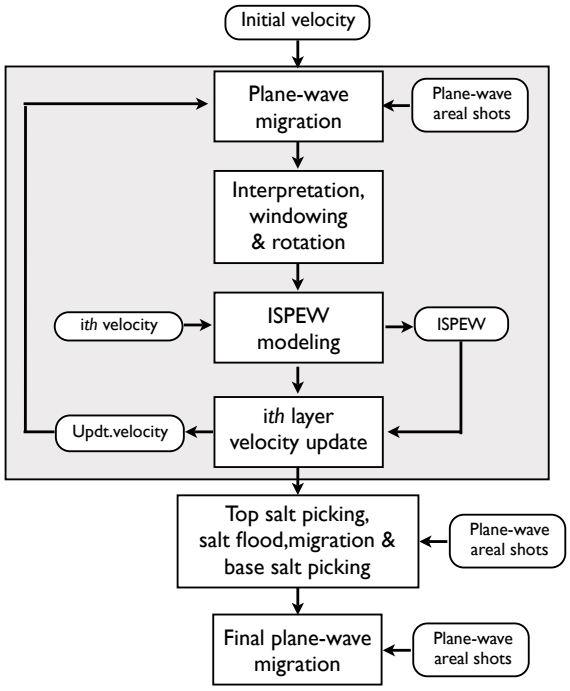

Figure 4: BP benchmark velocity model – Selected portion where shallow low-velocity anomalies occur.

update of the chalk layer, a reflector close to its base was interpreted on an initial prestack image computed with the initial velocity model. The choice of this reflector was motivated by its stronger signal-to-noise ratio and better continuity than the base of chalk itself. The updated velocity was subsequently extrapolated down to the base of chalk.

Results

Here, I will compare the prestack images obtained with the initial and final velocity models. Also, I compare the final image with the image computed with the vertical slice taken from the velocity cube estimated with 3D horizon-based ray-tracing tomography. This last comparison may not be completely fair, but can give a sense of

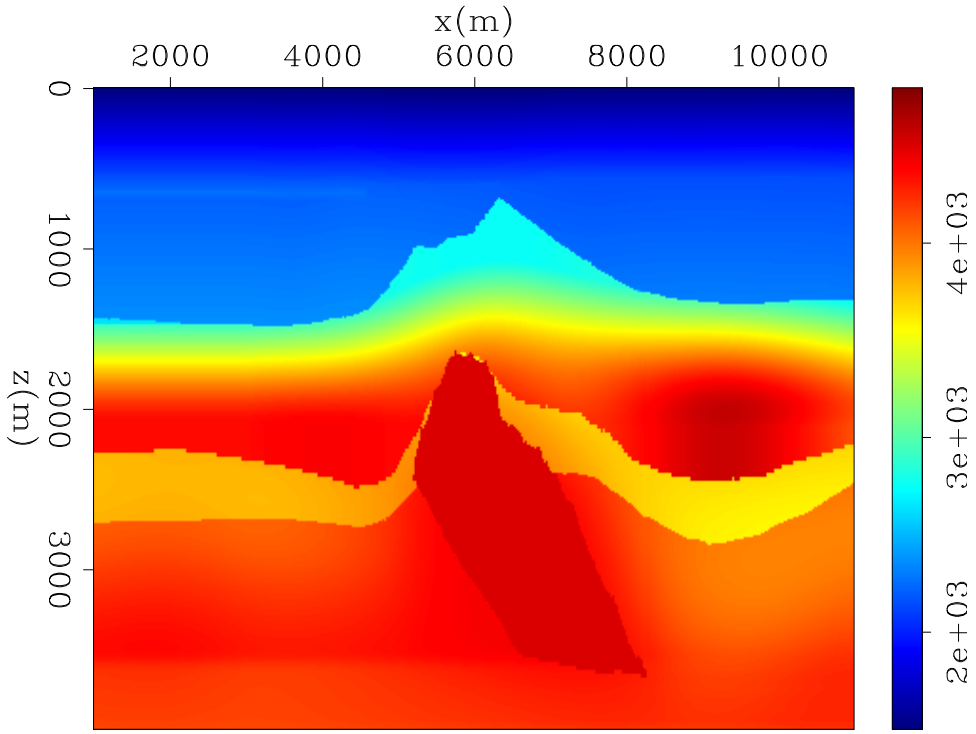

Figure 5: Final velocity model after edition of the salt body.

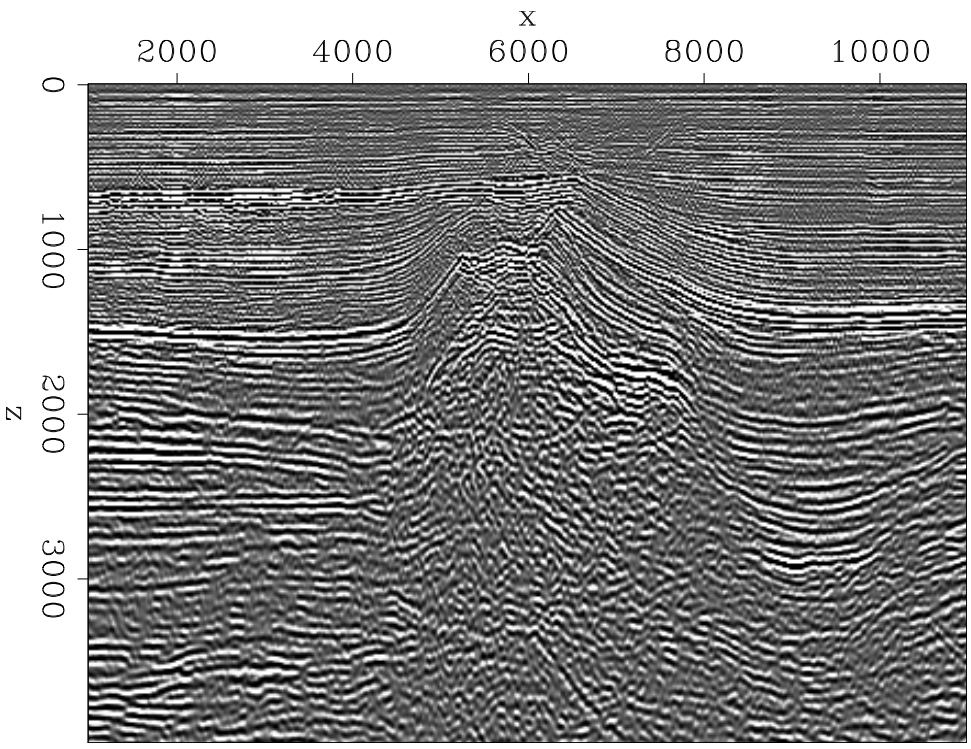

Figure 6: Image computed with the initial velocity model of Figure 2.

how close the final velocity computed with wave-equation tomography in the image space using ISPEW is to industry standards.

The comparison between the image computed with the initial velocity model (Figure 6) and the image computed with the final velocity model (Figure 7) shows better focusing of the reflectors, especially for the sediments on the left and on the right of the salt body. The angle gathers corroborate the greater accuracy of the final velocity model over the initial. Reflectors initially curving up in the angle gathers from the image computed with the initial velocity model(Figure 8) are flat in angle gathers from the image computed with the final velocity model (Figure 9). Also, by

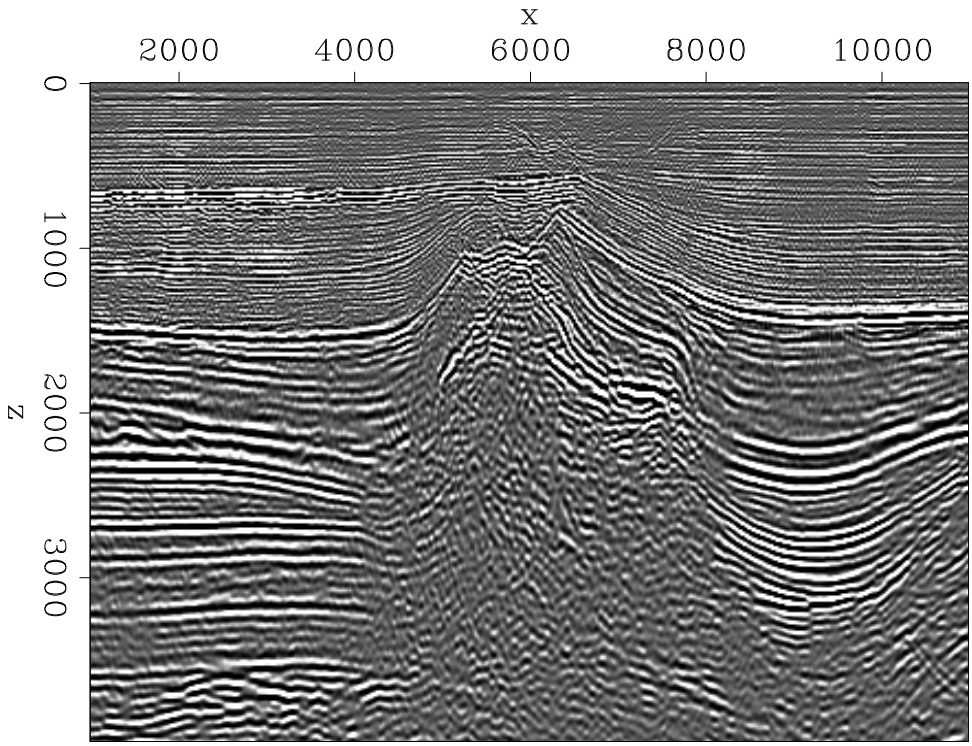

Figure 7: Image computed with the final velocity model of Figure 5.

comparing the image computed with the original velocity model (Figure 10) and the image computed with the final velocity model (Figure 7) one can see that, in general, the focusing of the reflectors and flatness of the angle gathers (Figures 9 and 11) is similar. A closer inspection, however, reveals that the pull-up that affects the image computed with the original velocity on the reflectors on the left of the salt body is not present in the image computed with the final velocity model. In addition, as can be seen in the zoomed images of Figures 12 and 13, reflectors are more continuous below the salt overhang in the image computed with the final velocity than that computed with the original velocity.

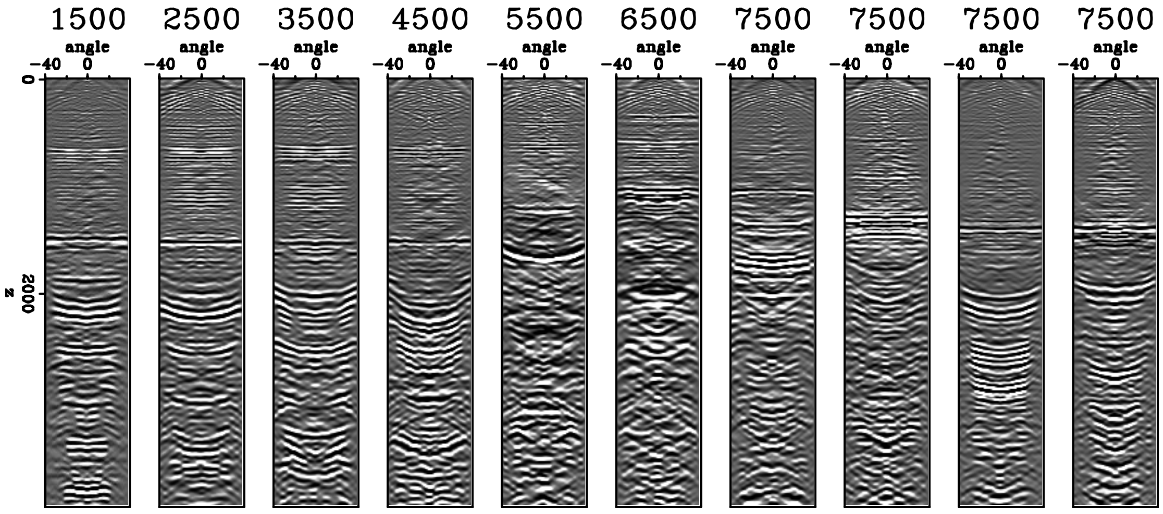

Figure 8: Angle gathers from the image computed with the initial velocity model of Figure 2.

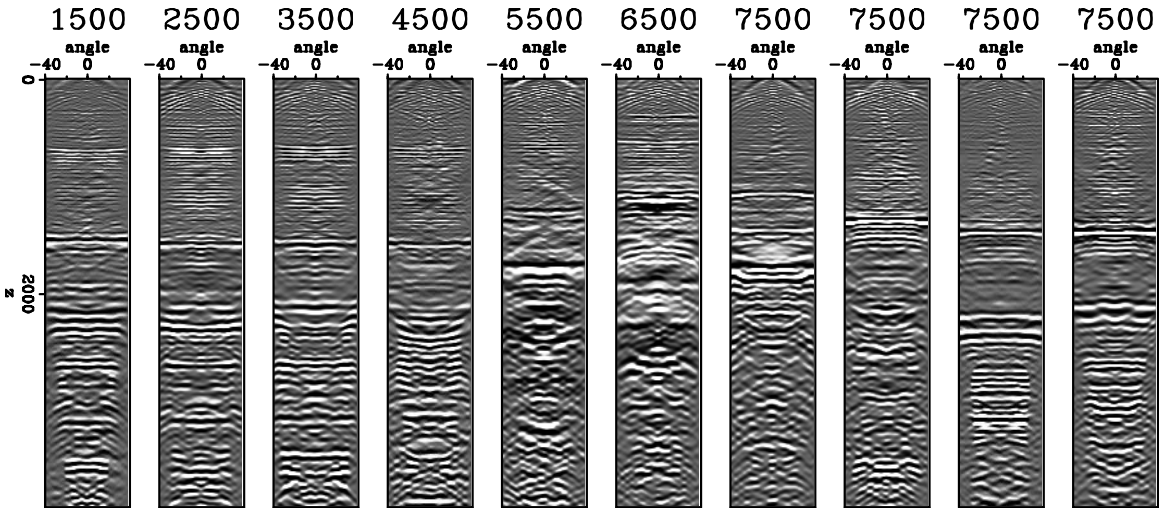

Figure 9: Angle gathers from the image computed with the final velocity model of Figure 5.

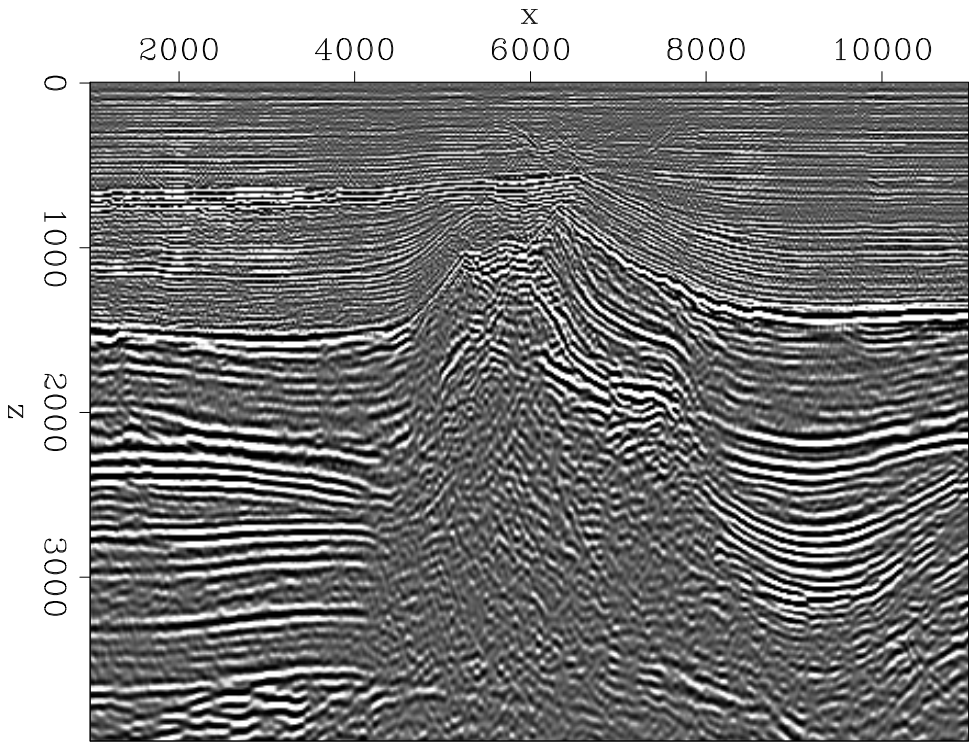

Figure 10: Image computed with the original velocity model of Figure 1.

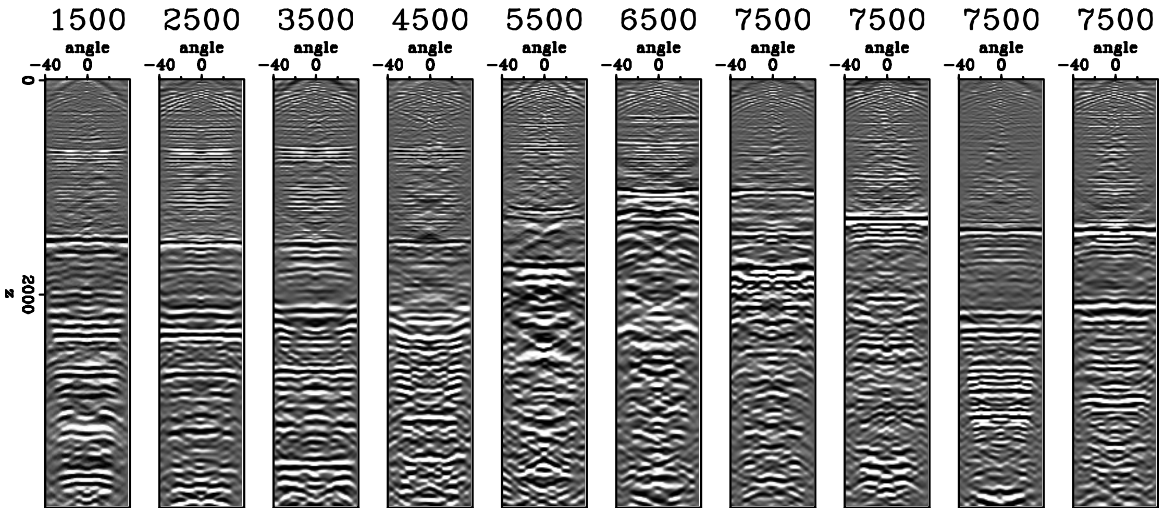

Figure 11: Angle gathers from the image computed with the original velocity model of Figure 1.

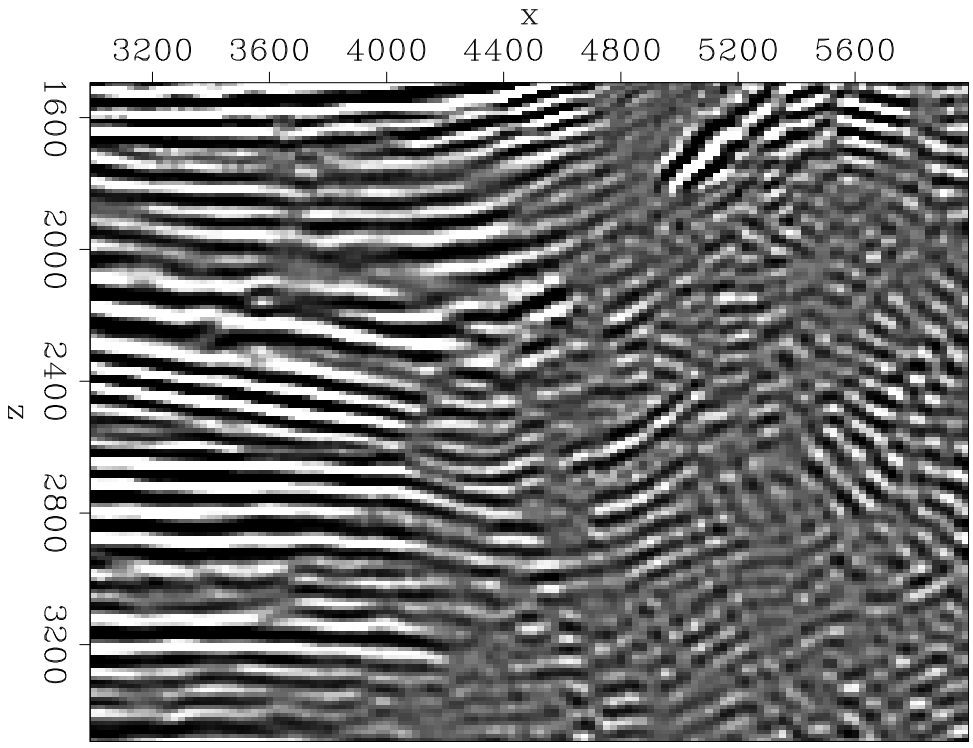

Figure 12: Zoomed version of Figure 7 in the salt overhang area.

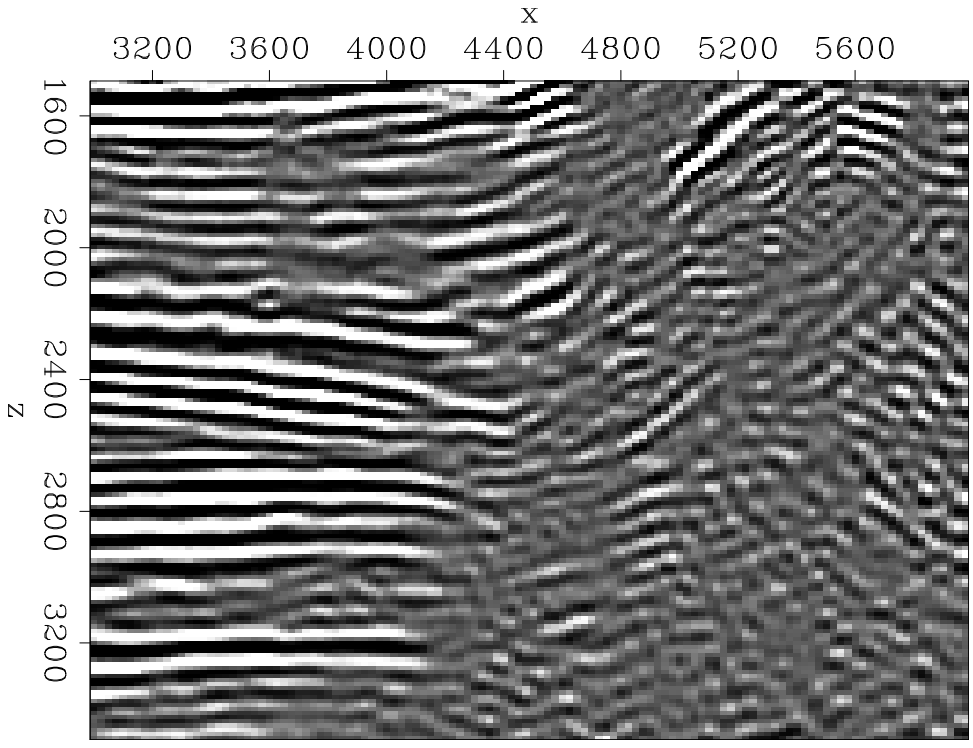

Figure 13: Zoomed version of Figure 10 in the salt overhang area.

INITIAL 3D COMMON-AZIMUTH MIGRATION

The 3D project on velocity model definition of the 3D Elf-North Sea dataset started on December, 7. Similarly, to the 2D project, velocity up to the top of chalk is considered sufficiently accurate, and smoothing and scaling was applied to the original 3D velocity model to generate the initial velocity model. After initial tests, migration was started on *cees – opteron* with 16 CPUs. The migration result can be seen in Figure 14. As can be noted, the subsurface-offset gathers are not focused at zero-offset for the shallow reflectors, which made me suspect that some parameterization was wrong. The common-azimuth migration program expects that offset is informed as half-offset. The header of the input data is in full-offset. Even though I correctly edited the information of the offset axis during the tests, I forgot to edit the header of the input data to inform the half-offset instead of full offset. The dataset used during the test phase are different from the ones used in the full migration. As CEES computers will be turned-off from Dec, 12, to Jan, 04, I will try to use SEP clusters in the meanwhile to generate the correct 3D initial image.

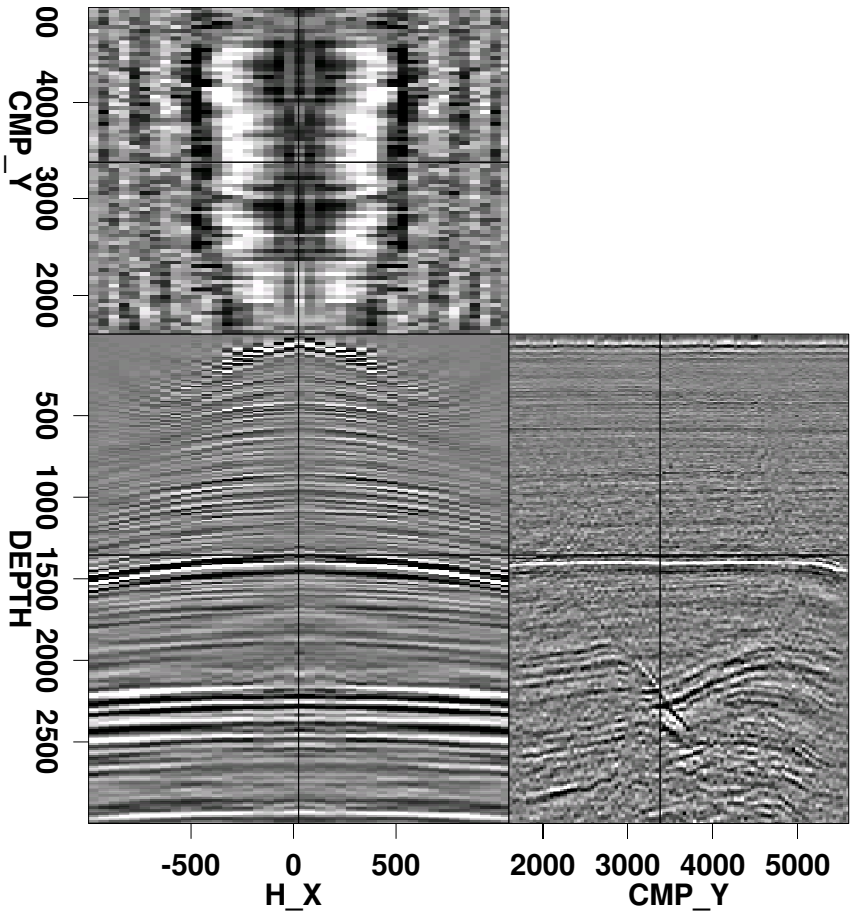

Figure 14: Incorrect 3D initial image od the 3D-Elf-North Sea.